HHS Public Access

Author manuscript

Neurochem Res. Author manuscript; available in PMC 2022 December 06.

Published in final edited form as:

Neurochem Res. 2021 November ; 46(11): 2979–2990. doi:10.1007/s11064-021-03401-2.

Protective Effects of Estrogen via Nanoparticle Delivery to Attenuate Myelin Loss and Neuronal Death after Spinal Cord Injury

Azizul Haque[1], **Kelsey P. Drasites**[1,2,3], **April Cox**[2], **Mollie Capone**[1,2], **Ali I. Myatich**[1,2,3], **Ramsha Shams**[1,2,3], **Denise Matzelle**[2,4], **Dena P. Garner**[3], **Mikhail Bredikhin**[5], **Donald C. Shields**[2], **Alexey Vertegel**[5], **Naren L. Banik**[1,2,4,6]

[1]Department of Microbiology and Immunology, Medical University of South Carolina, 173 Ashley Avenue, Charleston, SC 29425, USA

[2]Department of Neurosurgery, Medical University of South Carolina, 96 Jonathan Lucas Street, Charleston, USA

[3]Department of Health and Human Performance, The Citadel, 171 Moultrie St, Charleston, SC 29409, USA

[4]Ralph H. Johnson Veterans Administration Medical Center, 109 Bee St, Charleston, SC 29401, USA

[5]Department of Bioengineering, Clemson University, Clemson, SC, USA

[6]Department of Neurosurgery and Neurology, Medical University of South Carolina, 96 Jonathan Lucas Street, Charleston, SC 29425, USA

Abstract

Spinal cord injury (SCI) is associated with devastating neurological deficits affecting more than 11,000 Americans each year. Although several therapeutic agents have been proposed and tested, no FDA-approved pharmacotherapy is available for SCI treatment. We have recently demonstrated that estrogen (E2) acts as an antioxidant and anti-inflammatory agent, attenuating gliosis in SCI. We have also demonstrated that nanoparticle-mediated focal delivery of E2 to the injured spinal cord decreases lesion size, reactive gliosis, and glial scar formation. The current study tested in vitro effects of E2 on reactive oxygen species (ROS) and calpain activity in microglia, astroglia, macrophages, and fibroblasts, which are believed to participate in the inflammatory events and glial scar formation after SCI. E2 treatment decreased ROS production and calpain activity in these glial cells, macrophages, and fibroblast cells in vitro. This study also tested the efficacy of fast- and slow–release nanoparticle-E2 constructs in a rat model of SCI. Focal delivery of E2 via nanoparticles increased tissue distribution of E2 over time, attenuated cell death, and improved

✉Azizul Haque, haque@musc.edu, Naren L. Banik, baniknl@musc.edu.

Author Contributions AH conceived, designed, and wrote the manuscript, drew most of the figures, and edited the manuscript. KPD, AC, MC, AIM, and RS performed the experiments, prepared some of the figures, and edited the manuscript. DM performed spinal cord injury experiments, collected samples for analyses, and edited the manuscript. DPG and DCS edited the manuscript. MB and AV made E2-nanoparticles for the experiments. NLB conceived, designed, and edited the manuscript. All authors reviewed and approved the final version of the manuscript.

Conflict of interest The authors have no financial conflicts of interest.

myelin preservation in injured spinal cord. Specifically, the fast-release nanoparticle-E2 construct reduced the Bax/Bcl-2 ratio in injured spinal cord tissues, and the slow-release nanoparticle-E2 construct prevented gliosis and penumbral demyelination distal to the lesion site. These data suggest this novel E2 delivery strategy to the lesion site may decrease inflammation and improve functional outcomes following SCI.

Keywords

Calpain; Gliosis; Myelination; Nanoparticle-estrogen; Neuronal death; Reactive oxygen species; Spinal cord injury

Introduction

Spinal cord injury (SCI) is a debilitating medical condition that can permanently impair motor and sensory function, with an associated devastating financial burden to patients [1]. Currently, no FDA-approved drug exists for the treatment of acute SCI. Methylprednisolone was widely used in the past in the setting of acute SCI, but this controversial therapeutic option did not receive FDA approval due to limited efficacy [2–6]. Without effective treatment, SCI leads to infiltration of numerous peripheral macrophages and neutrophils, which play a crucial role in the activation of endogenous cells throughout the secondary injury process [7]. SCI also results in rapid reactive oxygen species (ROS) production and oxidative damage, leading to neuronal dysfunction and cell death [8]. ROS and oxidative stress are believed to play an important role in the pathophysiology of SCI [9]. Thus, alleviating oxidative stress may be an effective therapeutic strategy.

Reactive astrogliosis is widely recognized as a pathological trait of SCI [10]. Inflammatory events in SCI increase the activities of calpains, leading to neurodegeneration. Fibroblasts are ubiquitous in peripheral connective tissues and organs, and these cells are the principal generators of stroma [11]. Within the central nervous system (CNS), fibroblast-like cells are mostly associated with the vasculature and contribute to the basal laminae. However, injury to the spinal cord can induce a marked fibroblast response, producing matrix components. These matrix components may inhibit neural regeneration directly and promote prolonged tissue remodeling via interaction with inflammatory cells. These stromal elements become spatially compartmentalized by surrounding reactive astrocytes to form the fibrotic core of the spinal injury scar [12].

The glial scar is one of the primary impediments to regeneration and repair in the injured spinal cord. It is comprised of a number of components such as extracellular matrix proteins (ECM), activated astrocytes/microglia, fibroblasts, infiltrating immune cells, and axonal growth inhibitors. Two types of glial scar have been reported: glial and fibrous [13]. An important factor in the glial scar is chondroitin sulfate proteoglycan (CSPG), which is produced by activated glia, and serves to block axonal regrowth [14]. CSPGs are produced by activated astrocytes in response to the pro-inflammatory milieu present in the secondary injury setting [15]. Astrocytes, in particular, also form the glial scar predominately through hypertrophied processes [16]. One approach to decreasing the glial scar may therefore be to decrease astrocyte activation and proliferation. The steroid hormone estrogen (E2) has been

shown to decrease astrocytic glial fibrillary acidic protein (GFAP) expression in acute SCI [17–20]. Thus, focal delivery of E2 to the injured spinal cord may help prevent activation and proliferation of reactive gliosis-attenuating glial scar and axonal damage in SCI.

We have recently demonstrated that focal delivery of E2 via nanoparticles reduced gliosis and CSPG in acute/subacute phases of SCI, improving functional outcomes in a rat model of SCI [21]. However, the fibrotic scar also consists of ECM proteins such as fibronectin, collagen, and laminin that are secreted by infiltrating activated fibroblasts [22, 23]. Vimentin, an abundant cytoskeletal protein in cells of mesenchymal origin, has been associated with increased invasiveness and excessive scarring [24]. Inhibiting vimentin protects from fibrotic injuries [23, 25].

The use of single-agent targeted therapeutics in an enormously complex pathophysiology that includes inflammation, oxidative stress, protease activation, and glial scarring has not proven efficacious. Thus, evaluation of broadly acting agents, like E2, may be more effective. E2 is a highly pleiotropic substance that has been reported to activate transcription of some 137 E2 regulated genes [26]; E2 is known to have anti-inflammatory, anti-oxidant, anti-apoptotic, and neurotrophic properties [27–33]. E2 is also angiogenic and has exhibited a neuroprotective effect not only in SCI models [17, 32, 34–40] but also in experimental traumatic brain injury [41–46] and stroke models [47–51]. However, short-term systemic E2 treatment for contraception has been associated with increased risks of venous thromboembolism [52]. These safety concerns with traditional systemic E2 dosing (tablet or intravenous injection) are amplified in mobility-impaired SCI individuals who are already at an elevated risk for venous thromboembolism. Site-directed delivery through the use of nanoparticles provides for a significant reduction in systemic dosage, thereby reducing safety concerns. Such administration of low dose E2 via nanoparticles in SCI has been found to maintain E2 serum concentrations at physiological levels [21, 53].

Nanoparticles, synthetic polymers capable of targeted drug delivery, first received FDA approval for the treatment of cancer with Doxil in 1995 [54]. Subsequently, nanoparticle drug delivery systems have been shown to improve the therapeutic index of drugs. A recent exploratory delivery technique using methylprednisolone-loaded nanoparticles in a gel preparation was placed directly onto lesioned tissue in a rat SCI model, and its success illustrated the feasibility of this drug delivery approach [55]. Since acute SCI patients may undergo spine stabilization surgery, delivery of the nanoparticles directly via a surgically implanted epidural gel patch may effectively increase the therapeutic window of E2. This study therefore formulated and tested two different E2-nanoparticle constructs and examined their effects on gliosis and neuronal death in a rat model of SCI. Results from in vitro studies suggest that low dose E2 inhibits ROS, calpain activity, and vimentin production by fibroblast cells. In vivo studies suggest that focal delivery of E2 via nanoparticles attenuates glial activation, protects neuronal cells, and improves myelination and motor function in SCI.

Materials and Methods

Cell Lines

Mouse BV-2 microglia cells [56] were cultured in complete IMDM (Iscove's Modified Dulbecco's modified Eagle's medium) with 10% bovine growth serum (BGS) (Thermo Scientific, Logan, UT), 50 U/mL penicillin, and 50 μg/mL streptomycin (Life Technologies). Rat C6 astrocyte-like cell line was purchased from the BCRC (Bioresource Collection and Research Center; Taiwan) [57]. C6 cells were cultured in complete IMDM with 10% BGS (Thermo Scientific, Logan, UT), 50 U/mL penicillin, and 50 μg/mL streptomycin (Life Technologies) as described above. Mouse Raw264.7 macrophage cells [58] were cultured in complete DMEM (Dulbecco's modified Eagle's medium) with high glucose (Gibco, Thermo Scientific, Logan, Ut.) containing 10% fetal bovine serum (FBS) (Life Technologies), 50 U/mL penicillin, and 50 μg/mL streptomycin (Life Technologies). Human fibroblast M1 cells were cultured in complete DMEM (Corning, Manassas, VA) with 10% FBS (Thermo Scientific, Logan, UT), 50 U/mL penicillin, 50 μg/mL streptomycin (Life Technologies), and L-glutamate (Cellgro) as described [58]. Cells were cultured in a humidified incubator at 37 °C with 5% CO_2.

Reactive Oxygen Species (ROS) Detection Assay

BV-2, C6, Raw264.7, and M1 cells were cultured in complete media in tissue culture plates until 80% confluency. Cells were collected, counted, and 5×10^4 cells were treated with 40 ng/mL of IFN-γ in the presence or absence of 40 nM of E2 for 24 h in 96-well plates (200 μl/well). ROS was detected using Reactive Oxygen Species Assay Kit (Abcam ab186029) following the manufacturer's protocol. Fluorescence was measured at Ex/Em 650/675 after 30 min of incubation. Data analysis was performed using Microsoft Excel.

Calpain-Glo Protease Assay

Cells (4×10^6) were treated with 40 ng/mL of IFN-γ in the presence or absence of 40 nM of E2 for 24 h in 25 mL tissue culture flasks containing 5 mL of media. Cells were collected, washed in PBS three times, and lysed in complete lysis buffer on ice. From each batch, 100 μg of protein were used for assay. The assay was performed in triplicate in 96-well flat-bottomed plates using Calpain-Glo™ Protease Assay Kit (Promega G8501, G8502) following manufacturer's instructions. Plates were incubated at 37 °C for 5 min as indicated. Luminescence reading was recorded 10 min after the detection reagent was added. Data analysis was performed using Microsoft Excel.

Immunofluorescence

M1 cells were cultured on poly-D-lysine-coated (Sigma-Aldrich) coverslips, fixed with 4% paraformaldehyde (Sigma-Aldrich) in PBS (pH 7.4) for 10 min, washed three times with PBS, and incubated with blocking buffer containing 10% normal goat serum (Life Technologies) in PBS and 0.1% Triton X-100 for 30 min at room temperature. After removing the blocking buffer, cells were incubated overnight with primary antibodies against vimentin (1:500, Abcam ab92547) and GFAP (1:200, mouse monoclonal; Sigma-Aldrich-Aldrich Cat# G3893) at 4 °C. After washing three times with PBS at room

temperature, cells were incubated with fluorophore-conjugated secondary antibodies (Sigma-Aldrich) that recognized primary antibodies. DAPI (Thermo Fisher Scientific) was used to label cell nuclei. Slides were mounted with 1 drop of Invitrogen™ ProLong™ Gold Anti-fade Mountant with DAPI (Thermo Fisher Scientific) and cover slipped. After staining, cells were viewed under a fluorescence microscope with representative images taken at × 20 magnification.

Induction of SCI

Adult male Sprague-Dawley rats (200–250 g) were used for the induction of SCI and treatment with nanoparticle-encapsulated E2. While gender-related differences may be found in SCI where females are favored in terms of tissue preservation and locomotor recovery [60], no significant differences between males and females could be seen in SCI regarding the localization, onset, or distribution of pain. Moreover, factors affecting number of painful body regions, pain descriptors, ratings of pain intensities, and life satisfaction were similar. Thus, male rats were used in this study. Rats were anesthetized with ketamine (80 mg/kg)/xylazine (10 mg/kg). Following anesthetization of the animal and preparation of the surgical site, a midline incision was made on the back over the spinous processes, and a T-10 laminectomy was performed. SCI induction was performed as previously described [18, 61]. Briefly, the spine was immobilized with a stereotactic device, and the injury was induced via the method of Perot: dropping a constant weight (5 g) from a height of 8 cm onto an impounder (0.3 cm in diameter) gently placed on the spinal cord.

Vehicle-treated animals received the same volume of void nanoparticles in buffer (100 μL). Sham animals underwent a T-10 laminectomy [17, 18]. Wounds were closed using 5–0 absorbable suture (for interior wound closure). Exterior wound closure was performed with either 4–0 ethilon sutures or application of staples 5–8 mm apart (EZ-Clip wound clips). The surgical site was monitored, and based on the rate of healing, sutures are removed under isoflurane anesthesia.

After surgery, animals were placed on a warming pad until awake. Food was placed on the floor of the cage, and long-stemmed water bottles were provided for ease of access to water. Animals were checked twice daily until sacrifice. Animals were visually inspected to check for abnormal behaviors (head pressing, piloerection, hunching) and handled gently for closer physical inspection, including checking for bladder function. The animals' bladders were monitored and expressed twice daily. Rodents that develop urine scald were bathed with warm water and gently dried. Vaseline was applied to the affected area. Urine was expressed onto a clear glass dish in order to visually check for cloudiness.

If the subjects were not recovering appropriately, monitoring was amplified commensurate with the animal's health needs. Affected animals were thus treated with antibiotics or analgesics, given soft food, or placed on a heating pad, depending on the symptoms. Blood and tissue samples were collected 7–14 days post-injury. All animal experiments were performed in accordance with the *Guide for the Care and Use of Laboratory Animals* of the US Department of Health and Human Services (National Institutes of Health, Bethesda, MD, USA) and were approved by the Institutional Animal Care and Use Committee (IACUC) at the Medical University of South Carolina under the protocol ARC #1254.

Preparation of E2-loaded Fast and Slow Release Nanoparticles

Nanoparticles were formulated in the Bioengineering Department of Clemson University, South Carolina using the nanoprecipitation method previously described [62, 63]. E2-loaded nanoparticles were prepared according to the revised protocol [63]. In the case of PLGA (poly-lactic-co-glycolic acid) nanoparticles, 20 mg of 50:50 PGA-PLA co-polymer (PLGA), 5 mg of PLA:PEG, and 5 mg of E2 were dissolved in 2 mL of acetone. The resulting acetone solution was then added dropwise to 20 mL of deionized water, followed by ultrasonication in a bath sonicator (5510 Bransonic® Tabletop cleaner, Branson, Danbury, CT) for 30 min. To remove reagent residues, the obtained samples were centrifuged three times at 7000 RCF for 2 h and rinsed with PBS. In the case of PLA nanoparticles, 20 mg of pure PLA were used instead of 50:50 PLGA co-polymer. Each batch was evaluated for particle size (dynamic light scattering), load efficiency, and zeta potential to ensure consistency among batches. Nanoparticles were stored in sucrose at − 20 °C. Unloaded nanoparticles were also synthesized and used as a reference.

PLA nanoparticles, due to their higher hydrophobicity and slower degradation rate, have been previously shown to have slower drug release rate than PLGA nanoparticles [64]. Among different compositions of PLGA co-polymers, 50:50 PLGA formulation has been previously shown to possess the fastest drug release rate [65]. Thus, pure PLA and 50:50 PLGA were used here as the two formulations capable of providing slow and fast drug release rates, respectively.

Gel Plug Delivery System

Gel plugs (0.6% SeaPlaque agarose in PBS) were made by dissolving lyophilized E2-loaded PLGA nanoparticles at either 25 or 2.5 μg dose (or saline loaded vehicle control) in 50 μL sterile filtered PBS. The gel (final volume 50 μL) was set in PCR amplification tubes overnight to harden. Prior to insertion into animals, gels were sterilized under a tissue culture UV lamp for 15 min.

Measurement of E2 Concentrations in Spinal Cord Tissues and Plasma by ELISA

Spinal cord tissue homogenates from PLGA-E2 treatment group were diluted 1:10–1:100 in 6% BSA block. Plasma samples from PLA-E2 treatment group were serially diluted and used in the assay. E2 concentration was determined using a commercially available ELISA kit (Calbiotech Estradiol ELISA ES180S) [21]. Undiluted samples were processed following directions provided by the manufacturer. Using protein concentration data gathered from Bradford assay, the tissue sample E2 concentration was then converted from pg/mL to pg/μg of total protein to account for differences in protein concentrations between samples. Plasma E2 concentrations were expressed as pg/ml.

Western Blot Analysis

Spinal cord samples were homogenized on ice in a standard homogenizing buffer (50 mM Tris-HCl, pH 7.4; 5 mM EGTA; 1 mM phenylmethylsulfonyl fluoride) with protease inhibitor as described [66–68]. Equal protein concentrations (30 μg/lane) from designated samples were separated on a 4–12% Bis/Tris NuPage gel (Invitrogen, Grand Island, NY) [69–71]. Proteins were transferred onto a nitrocellulose membrane (Pierce, Rockford IL),

and the blot was probed with Bcl-2 (Santa Cruz Biotechnology, sc-7382), Bax (Santa Cruz, sc-7480), Iba-1 (Abcam, ab153696), GFAP (Invitrogen, 14-9892-82), and MBP (1:1000, Millipore, MAB384), and Vimentin (1:1000, Abcam, ab92547). antibodies. The secondary antibodies used were horseradish peroxidase conjugated anti-mouse (1:2000, Santa Cruz, sc-2005) and anti-rabbit (1:4000, Santa Cruz, sc-2004). A monoclonal antibody for β-actin (1:1000, Santa Cruz, sc-81,178) was used as a protein loading control. Relative protein expression was assessed using Image J software (National Institutes of Health, Bethesda, MD) and expressed as relative density for each sample [72–74].

Statistical Analysis

Statistical analyses were performed using Microsoft Excel and GraphPad Prism (version 6.0) Software. The immunoreactive bands obtained from Western blotting and the immunoreactive pixels of the immunofluorescence data were analyzed with ImageJ software (U.S. National Institutes of Health, Bethesda, MD). Two-tailed paired t-test and one-way ANOVA with Bonferroni test for multiple comparisons were used to determine statistical significance for all other analyses. Data were expressed as mean ± SEM or mean+/STDEV. A p-value < 0.05 was determined to be statistically significant for all calculations.

Results

Low Dose E2 Treatment Attenuates ROS Production by Microglia, Astroglia, Macrophages, and Fibroblast Cells

To determine the effects of E2 on ROS production, cells (microglia, astroglia, macrophages, and fibroblast) were treated with IFN-γ plus or minus E2 (40 nM) and tested for cellular ROS using Reactive Oxygen Species Assay Kit as described in the methods. Treatment of cells with IFN-γ significantly elevated ROS levels ($p < 0.05$) in microglia, astroglia, and fibroblast cells (Fig. 1A, B, and D). The production of ROS was also markedly elevated in 264.7 Raw macrophage cells, but it was not statistically significant (Fig. 1C). Strikingly, E2 treatment significantly inhibited ROS production in all the cells tested in the presence of IFN-γ (Fig. 1). These data suggest that low dose E2 attenuates cellular damage in glial cells, macrophages, and fibroblasts.

Low Dose E2 Treatment Attenuates Calpain Activity in Microglia, Astroglia, Macrophages, and Fibroblast Cells

To examine the effects of low dose E2 (40 nM) on calpain activity in macrophages, fibroblasts, and glial cells, cells were treated with or without IFN-γ as described in the methods. Treatment of cells with IFN-γ significantly increased calpain activity ($p < 0.05$) in microglia, astroglia, and fibroblast cells (Fig. 2A, B, and D). An increased calpain activity was also detected in 264.7 Raw macrophage cells, but it was not statistically significant (Fig. 2C). Interestingly, E2 treatment significantly inhibited calpain activity in all the cells tested in the presence of IFN-γ (Fig. 2). These data suggest that low dose E2 attenuates calpain activity, which may in turn reduce inflammatory events in glial cells, macrophages, and fibroblasts.

Low Dose E2 Treatment Decreases Vimentin Expression in Fibroblast Cells

Vimentin has been shown to be involved in wound healing, but its functional contribution to this process is poorly understood. Loss of vimentin may lead to a severe deficiency in fibroblast growth. While astrocytic scars may act as a physical barrier to axonal growth, fibroblasts can play a role in the complex process of axonal growth. Glial fibrillary acidic protein (GFAP) and vimentin mediates reactive astrogliosis and glial scar formation. We have previously shown that E2 attenuates glial scarring after SCI [21]. In this study, we examined vimentin expression levels in IFN-γ activated fibroblast cells by immunohistochemistry and western blotting (Fig. 3). Treatment of fibroblast cells with low dose E2 (5–50 nM) reduced Vimentin level as analyzed by immunohistochemistry (Fig. 3A). A significant reduction of vimentin expression in fibroblast cells was noted when the fluorescence intensity was analyzed by one-way ANOVA (Fig. 3B). Similarly, western blot analyses showed that the expression of Vimentin was significantly decreased by low dose E2 (Fig. 3C and D). These in vitro findings align with our earlier results from an acute model of SCI and suggest that E2 treatment may reduce complex glial scar formation in SCI.

Bioavailability of Fast and Slow Release E2 Embedded Nanoparticles in SCI Rats

Our recent study has shown E2 driven neuroprotection in experimental SCI following systemic administration [75]. While systematic delivery of E2 reduces inflammation and improves functional outcome, it also causes thrombotic sequelae. Thus, we have formulated fast (PLGA-E2) and slow (PLA-E2) release nanoparticle E2 constructs (Fig. 4) to increase tissue concentration and reduce inflammation and neuronal death after SCI. The release of E2 was tested at various time points to confirm fast (Fig. 4A) and slow (Fig. 4B) release E2 embedded nanoparticles can be administered using a gel patch. Rapid release of PLGA-E2 gel patches (5.0 μg dose) were surgically placed on lesioned spinal cords. Animals were euthanized at 48 h following SCI induction and patch placement. Spinal cord tissue was collected at necropsy and analyzed for E2 concentrations by ELISA. Fast release PLGA-E2 gel patch resulted in decreased plasma concentrations [21] with increased tissue concentrations (Fig. 4C).

On the other hand, slow release PLA-E2 gel patches (5.0 μg dose) were surgically implanted in the acute rat SCI model. Animals were euthanized at day 0, 1, 2, 3 and 7 following SCI induction and patch placement. Blood plasma sample was collected after sacrifice and analyzed for E2 concentrations by ELISA. Slow release PLA-E2 gel patch also resulted in low plasma E2 concentrations (Fig. 4D). These data suggest that these focal E2 delivery approaches in the injured spinal may help attenuate inflammatory responses after SCI.

Focal Delivery of Fast Release PLGA-E2 Alters Bax/Bcl-2 Ratio and Protect Cells in Injured Spinal Cord

Bcl-2 family members mediate apoptotic signals through pro-apoptotic protein Bax and anti-apoptotic protein Bcl-2. The ratio of Bax and Bcl-2 is believed to be increased in spinal cord tissues following SCI [76]. Our western blot analysis showed that the expression of Bax was decreased while the expression of the Bcl-2 protein was increased in PLGA-E2 treated rats after SCI (Fig. 5). These data suggest that focal delivery of E2 via fast release nanoparticles protects neuronal cells in SCI.

Focal Delivery of Slow Release PLA-E2 Improves Myelination in Injured Spinal Cord

Secondary inflammation after SCI often promotes demyelination, impacting the recovery of neurological function. Thus, the effects of PLA-E2 on myelin basic protein (MBP) expression in injured spinal cord were also tested by western blotting, demonstrating increased levels of MBP in treated rats (Fig. 6). E2 may therefore attenuate demyelination in injured spinal cord.

Focal Delivery of Slow Release PLA-E2 Reduces Gliosis in Injured Spinal Cord

The activation of microglia/astrocytes is often detected following SCI. Here, we tested spinal cord tissues from the injured section following SCI and gel patch therapy with PLA-E2. Western blot analysis showed that microglial marker Iba-1 and astroglial marker GFAP were significantly reduced following focal delivery of E2 via PLA-E2 (Fig. 7). These data suggest that slow release E2 is effective in reducing glial activation in SCI.

Discussion

We have recently shown that E2 treatment reduces CSPG formation after SCI [21]. Injury to the spinal cord induces a significant fibroblast response which produces matrix components [77]. These matrix components may inhibit neural regeneration directly and promote prolonged tissue remodeling via interactions with inflammatory cells. SCI triggers a complex cascade of events that culminates in the spinal injury scar, consisting of multiple cell types and extracellular, non-neural components [78]. The lack of repair following SCI is due to both cell intrinsic factors and the extrinsic injury microenvironment. ROS regulate cellular homeostasis and act as prime modulators of cellular dysfunction contributing to disease pathophysiology. ROS are generated during mitochondrial oxidative metabolism as well as in cellular response to insults. Oxidative stress due to excess ROS is implicated in various neurodegenerative diseases.

Using microglia, astroglia, macrophages, and fibroblast cell lines, we have shown that IFN-γ induces ROS and increases calpain activity; however, both are significantly reduced by E2 administration. In a human fibroblast cell line, we have shown that IFN-γ induces upregulation of the fibroblast activation marker, vimentin. E2 treatment decreased vimentin immunoreactivity, suggesting that E2 can modulate fibroblast activation. This also suggests that E2 treatment in the chronic stage of SCI may alter glial and fibroblast activation with subsequent effects on glial scar composition. The pathophysiology of SCI is characterized by an initial primary injury to the spinal cord followed by a secondary phase of injury. In severe SCI, secondary lesions include activation of an inflammatory cascade and overproduction of free radicals, with overall poor outcomes [79–81]. Although the etiology and pathogenesis of secondary injury processes remain to be fully understood, it has been suggested that the production of ROS and oxidative stress play a significant role in SCI pathophysiology. Thus, reducing ROS and oxidative stress-mediated secondary injury process may provide an effective strategy for therapeutic intervention of SCI. Tissue degeneration can be initiated by cell membrane injury, inflammation, axonal damage, ROS, reactive free radicals, accumulation of calcium, and excessive calpain activity in cells. Focal

delivery of E2 may attenuate these events in injured spinal cord tissues, protecting neurons and improving functional outcome.

The ROS formed under normal physiological conditions may have both beneficial and harmful functions [82]. ROS promote apoptosis of vascular and neuronal cells and stimulate inflammation - while also supporting angiogenesis. Mitochondria are the major source of ROS in fibroblasts, which are thought to be crucial regulators of wound healing. Like many biologically active substances with antioxidant properties, low dose E2 may act as an anti-inflammatory agent to reduce ROS and oxidative stress. In the CNS, microglial cells are likely the main source of ROS production. Thus, microglial ROS production by IFN-γ was tested first; however, activated astrocytes, macrophages, and fibroblasts also appear to generate ROS. Accumulating evidence also suggests that ROS serves as critical signaling molecules in cell proliferation and survival [83–85]. Oxidative stress results in direct or indirect ROS-mediated damage of nucleic acids, proteins, and lipids, and it has been implicated in neurodegeneration [86, 87]. Because ROS are important mediators for activation of pro-inflammatory signaling pathways, inhibition of ROS by E2 may regulate inflammation following SCI.

Vimentin also plays an important role in inflammatory cell migration. Loss of vimentin may lead to a severe deficiency in fibroblast growth, limiting its role in glial scar formation. However, vimentin can also participate in many processes crucial for tissue repair and regeneration, including cell migration, proliferation, differentiation, angiogenesis, extracellular matrix remodeling, and immune responses [88]. E2 treatment reduced vimentin expression in fibroblast cells, and calpain activity was also significantly decreased. Excessive calcium levels after injury may result in the activation of calpains, which can promote oxidation of fatty acids in cell membranes and demyelination. Reduction of calpain activity was observed in glial cells, macrophages, and fibroblasts following E2 treatment. Interestingly, E2 treatment also induced protection of myelin in SCI rats, suggesting that demyelination can be minimized by E2 after SCI.

Reactive astrocytes play a role in pathological processes following SCI [89]. Even in the normal aging brain, reactive astrocytes are thought to contribute to inflammatory processes [90]. These cells form a physical barrier to obstruct axonal growth and secrete inhibitory proteins that hinder functional recovery. During the chronic phase of SCI, astrocytes may transform into scar-forming astrocytes [78, 90], which produce inhibitory factors such as CSPG [89]. This was significantly attenuated by rapid release PLGA-E2 treatment. Thus, the above data indicates slow release PLA-E2 significantly reduced microglial/astroglial activation, suggesting nanoparticle mediated delivery of E2 is effective against glial activation and inflammatory responses following SCI. Therefore, all these factors taken together E2 treatment may facilitate the pathway for regeneration process required in damaged axon for making connection following SCI.

Acknowledgements

This work was supported in part by funding from the Veterans Administration (1IOBX001262, 1I01BX002349-01, 2I01 BX001262-05, 1I01 BX004269-01), South Carolina State Spinal Cord Injury Research Fund (SCIRF-2015P-01, SCIRF-2015P-04, SCIRF-2015-I-01, SCIRF #2016 I-03, and SCIRF #2018 I-01). Contents

do not necessarily represent the policy of the SCIRF and do not imply endorsement by the funding agency. This work was also supported in part by funding from the National Institutes of Health (1R21NS118393-01).

Data Availability

The data used to support the findings of this manuscript are available from the corresponding authors upon reasonable written request.

References

1. Upadhyayula PS, Martin JR, Rennert RC, Ciacci JD (2021) Review of operative considerations in spinal cord stem cell therapy. World Jo Stem Cells 13:168–176
2. Hall ED (2003) Drug development in spinal cord injury: what is the FDA looking for? J Rehabil Res Dev 40:81–91
3. Schroeder GD, Kwon BK, Eck JC, Savage JW, Hsu WK, Patel AA (2014) Survey of Cervical Spine Research Society members on the use of high-dose steroids for acute spinal cord injuries. Spine 39:971–977 [PubMed: 24583739]
4. Lammertse DP (2013) Clinical trials in spinal cord injury: lessons learned on the path to translation. The 2011 International Spinal Cord Society Sir Ludwig Guttmann Lecture. Spinal cord 51:2–9 [PubMed: 23165505]
5. Breslin K, Agrawal D (2012) The use of methylprednisolone in acute spinal cord injury: a review of the evidence, controversies, and recommendations. Pediatr Emerg Care 28:1238–1245; quiz 1246 – 1238 [PubMed: 23128657]
6. Bracken MB (2012) Steroids for acute spinal cord injury. Cochrane Database Syst Rev 1:CD001046 [PubMed: 22258943]
7. Zhou X, He X, Ren Y (2014) Function of microglia and macrophages in secondary damage after spinal cord injury. Neural Regener Res 9:1787–1795
8. Ge X, Tang P, Rong Y, Jiang D, Lu X, Ji C, Wang J, Huang C, Duan A, Liu Y, Chen X, Chen X, Xu Z, Wang F, Wang Z, Li X, Zhao W, Fan J, Liu W, Yin G, Cai W (2021) Exosomal miR-155 from M1-polarized macrophages promotes EndoMT and impairs mitochondrial function via activating NF-kappaB signaling pathway in vascular endothelial cells after traumatic spinal cord injury. Redox Biol 41:101932 [PubMed: 33714739]
9. Jia Z, Zhu H, Li J, Wang X, Misra H, Li Y (2012) Oxidative stress in spinal cord injury and antioxidant-based intervention. Spinal Cord 50:264–274 [PubMed: 21987065]
10. Karimi-Abdolrezaee S, Billakanti R (2012) Reactive astrogliosis after spinal cord injury-beneficial and detrimental effects. Mol Neurobiol 46:251–264 [PubMed: 22684804]
11. Tripathi M, Billet S, Bhowmick NA (2012) Understanding the role of stromal fibroblasts in cancer progression. Cell Adhes Migr 6:231–235
12. Soderblom C, Luo X, Blumenthal E, Bray E, Lyapichev K, Ramos J, Krishnan V, Lai-Hsu C, Park KK, Tsoulfas P, Lee JK (2013) Perivascular fibroblasts form the fibrotic scar after contusive spinal cord injury. J Neurosci 33:13882–13887 [PubMed: 23966707]
13. Leal-Filho MB (2011) Spinal cord injury: from inflammation to glial scar. Surg Neurol Int 2:112 [PubMed: 21886885]
14. Cregg JM, DePaul MA, Filous AR, Lang BT, Tran A, Silver J (2014) Functional regeneration beyond the glial scar. Exp Neurol 253:197–207 [PubMed: 24424280]
15. Siebert JR, Conta Steencken A, Osterhout DJ (2014) Chondroitin sulfate proteoglycans in the nervous system: inhibitors to repair. BioMed Res Int 2014:845323 [PubMed: 25309928]
16. Jurzak M, Adamczyk K, Antonczak P, Garncarczyk A, Kusmierz D, Latocha M (2014) Evaluation of genistein ability to modulate CTGF mRNA/protein expression, genes expression of TGFbeta isoforms and expression of selected genes regulating cell cycle in keloid fibroblasts in vitro. Acta Pol Pharm 71:972–986 [PubMed: 25745770]
17. Samantaray S, Smith JA, Das A, Matzelle DD, Varma AK, Ray SK, Banik NL (2011) Low dose estrogen prevents neuronal degeneration and microglial reactivity in an acute model of spinal cord

injury: effect of dosing, route of administration, and therapy delay. Neurochem Res 36:1809–1816 [PubMed: 21611834]

18. Sribnick EA, Wingrave JM, Matzelle DD, Wilford GG, Ray SK, Banik NL (2005) Estrogen attenuated markers of inflammation and decreased lesion volume in acute spinal cord injury in rats. J Neurosci Res 82:283–293 [PubMed: 16130149]
19. Schaufelberger SA, Rosselli M, Barchiesi F, Gillespie DG, Jackson EK, Dubey RK (2016) 2-Methoxyestradiol, an endogenous 17beta-estradiol metabolite, inhibits microglial proliferation and activation via an estrogen receptor-independent mechanism. Am J Physiol Endocrinol Metab 310:E313–E322 [PubMed: 26732685]
20. Samantaray S, Das A, Matzelle DC, Yu SP, Wei L, Varma A, Ray SK, Banik NL (2016) Administration of low dose estrogen attenuates gliosis and protects neurons in acute spinal cord injury in rats. J Neurochem 136:1064–1073 [PubMed: 26662641]
21. Cox A, Capone M, Matzelle D, Vertegel A, Bredikhin M, Varma A, Haque A, Shields DC, Banik NL (2021) Nanoparticle-based estrogen delivery to spinal cord injury site reduces local parenchymal destruction and improves functional recovery. J Neurotrauma 38:342–352 [PubMed: 32680442]
22. Shearer MC, Fawcett JW (2001) The astrocyte/meningeal cell interface—a barrier to successful nerve regeneration? Cell Tissue Res 305:267–273 [PubMed: 11545264]
23. Das SK, Gupta I, Cho YK, Zhang X, Uehara H, Muddana SK, Bernhisel AA, Archer B, Ambati BK (2014) Vimentin knockdown decreases corneal opacity. Investig Ophthalmol Vis Sci 55:4030–4040 [PubMed: 24854859]
24. Li H, Chang L, Du WW, Gupta S, Khorshidi A, Sefton M, Yang BB (2014) Anti-microRNA-378a enhances wound healing process by upregulating integrin beta-3 and vimentin. Mol Ther 22:1839–1850 [PubMed: 24954475]
25. dos Santos G, Rogel MR, Baker MA, Troken JR, Urich D, Morales-Nebreda L, Sennello JA, Kutuzov MA, Sitikov A, Davis JM, Lam AP, Cheresh P, Kamp D, Shumaker DK, Budinger GR, Ridge KM (2015) Vimentin regulates activation of the NLRP3 inflammasome. Nat Commun 6:6574 [PubMed: 25762200]
26. Lin CY, Strom A, Vega VB, Kong SL, Yeo AL, Thomsen JS, Chan WC, Doray B, Bangarusamy DK, Ramasamy A, Vergara LA, Tang S, Chong A, Bajic VB, Miller LD, Gustafsson JA, Liu ET (2004) Discovery of estrogen receptor alpha target genes and response elements in breast tumor cells. Genome Biol 5:R66 [PubMed: 15345050]
27. Sribnick EA, Ray SK, Banik NL (2004) Estrogen as a multi-active neuroprotective agent in traumatic injuries. Neurochem Res 29:2007–2014 [PubMed: 15662835]
28. Samantaray S, Sribnick EA, Das A, Thakore NP, Matzelle D, Yu SP, Ray SK, Wei L, Banik NL (2010) Neuroprotective efficacy of estrogen in experimental spinal cord injury in rats. Ann N Y Acad Sci 1199:90–94 [PubMed: 20633113]
29. Kipp M, Berger K, Clarner T, Dang J, Beyer C (2012) Sex steroids control neuroinflammatory processes in the brain: relevance for acute ischaemia and degenerative demyelination. J Neuroendocrinol 24:62–70 [PubMed: 21592237]
30. Evsen MS, Ozler A, Gocmez C, Varol S, Tunc SY, Akil E, Uzar E, Kaplan I (2013) Effects of estrogen, estrogen/progesteron combination and genistein treatments on oxidant/antioxidant status in the brain of ovariectomized rats. Eur Rev Med Pharmacol Sci 17:1869–1873 [PubMed: 23877849]
31. Kumar S, Lata K, Mukhopadhyay S, Mukherjee TK (2010) Role of estrogen receptors in pro-oxidative and anti-oxidative actions of estrogens: a perspective. Biochim Biophys Acta 1800:1127–1135 [PubMed: 20434525]
32. Cuzzocrea S, Genovese T, Mazzon E, Esposito E, Di Paola R, Muia C, Crisafulli C, Peli A, Bramanti P, Chaudry IH (2008) Effect of 17beta-estradiol on signal transduction pathways and secondary damage in experimental spinal cord trauma. Shock 29:362–371 [PubMed: 17704735]
33. Elkabes S, Nicot AB (2014) Sex steroids and neuroprotection in spinal cord injury: a review of preclinical investigations. Exp Neurol 259:28–37 [PubMed: 24440641]

34. Sribnick EA, Samantaray S, Das A, Smith J, Matzelle DD, Ray SK, Banik NL (2010) Postinjury estrogen treatment of chronic spinal cord injury improves locomotor function in rats. J Neurosci Res 88:1738–1750 [PubMed: 20091771]
35. Ritz MF, Hausmann ON (2008) Effect of 17beta-estradiol on functional outcome, release of cytokines, astrocyte reactivity and inflammatory spreading after spinal cord injury in male rats. Brain Res 1203:177–188 [PubMed: 18316064]
36. Mosquera L, Colon JM, Santiago JM, Torrado AI, Melendez M, Segarra AC, Rodriguez-Orengo JF, Miranda JD (2014) Tamoxifen and estradiol improved locomotor function and increased spared tissue in rats after spinal cord injury: their antioxidant effect and role of estrogen receptor alpha. Brain Res 1561:11–22 [PubMed: 24637260]
37. Lee JY, Choi SY, Oh TH, Yune TY (2012) 17beta-Estradiol inhibits apoptotic cell death of oligodendrocytes by inhibiting RhoA-JNK3 activation after spinal cord injury. Endocrinology 153:3815–3827 [PubMed: 22700771]
38. Yune TY, Kim SJ, Lee SM, Lee YK, Oh YJ, Kim YC, Markelonis GJ, Oh TH (2004) Systemic administration of 17beta-estradiol reduces apoptotic cell death and improves functional recovery following traumatic spinal cord injury in rats. J Neurotrauma 21:293–306 [PubMed: 15115604]
39. Siriphorn A, Dunham KA, Chompoopong S, Floyd CL (2012) Postinjury administration of 17beta-estradiol induces protection in the gray and white matter with associated functional recovery after cervical spinal cord injury in male rats. J Comp Neurol 520:2630–2646 [PubMed: 22684936]
40. Kachadroka S, Hall AM, Niedzielko TL, Chongthammakun S, Floyd CL (2010) Effect of endogenous androgens on 17beta-estradiol-mediated protection after spinal cord injury in male rats. J Neurotrauma 27:611–626 [PubMed: 20001688]
41. Day NL, Floyd CL, D'Alessandro TL, Hubbard WJ, Chaudry IH (2013) 17beta-estradiol confers protection after traumatic brain injury in the rat and involves activation of G protein-coupled estrogen receptor 1. J Neurotrauma 30:1531–1541 [PubMed: 23659385]
42. Zhang D, Hu Y, Sun Q, Zhao J, Cong Z, Liu H, Zhou M, Li K, Hang C (2013) Inhibition of transforming growth factor beta-activated kinase 1 confers neuroprotection after traumatic brain injury in rats. Neuroscience 238:209–217 [PubMed: 23485590]
43. Asl SZ, Khaksari M, Khachki AS, Shahrokhi N, Nourizade S (2013) Contribution of estrogen receptors alpha and beta in the brain response to traumatic brain injury. J Neurosurg 119:353–361 [PubMed: 23724987]
44. Gatson JW, Liu MM, Abdelfattah K, Wigginton JG, Smith S, Wolf S, Simpkins JW, Minei JP (2012) Estrone is neuroprotective in rats after traumatic brain injury. J Neurotrauma 29:2209–2219 [PubMed: 22435710]
45. Zlotnik A, Leibowitz A, Gurevich B, Ohayon S, Boyko M, Klein M, Knyazer B, Shapira Y, Teichberg VI (2012) Effect of estrogens on blood glutamate levels in relation to neurological outcome after TBI in male rats. Intens Care Med 38:137–144
46. Soustiel JF, Palzur E, Nevo O, Thaler I, Vlodavsky E (2005) Neuroprotective anti-apoptosis effect of estrogens in traumatic brain injury. J Neurotrauma 22:345–352 [PubMed: 15785230]
47. Perez-Alvarez MJ, Maza Mdel C, Anton M, Ordonez L, Wandosell F (2012) Post-ischemic estradiol treatment reduced glial response and triggers distinct cortical and hippocampal signaling in a rat model of cerebral ischemia. J Neuroinflamm 9:157
48. Ardelt AA, Carpenter RS, Lobo MR, Zeng H, Solanki RB, Zhang A, Kulesza P, Pike MM (2012) Estradiol modulates post-ischemic cerebral vascular remodeling and improves long-term functional outcome in a rat model of stroke. Brain Res 1461:76–86 [PubMed: 22572084]
49. Zhang QG, Raz L, Wang R, Han D, De Sevilla L, Yang F, Vadlamudi RK, Brann DW (2009) Estrogen attenuates ischemic oxidative damage via an estrogen receptor alpha-mediated inhibition of NADPH oxidase activation. J Neurosci 29:13823–13836 [PubMed: 19889994]
50. Lebesgue D, Chevaleyre V, Zukin RS, Etgen AM (2009) Estradiol rescues neurons from global ischemia-induced cell death: multiple cellular pathways of neuroprotection. Steroids 74:555–561 [PubMed: 19428444]
51. Merchenthaler I, Dellovade TL, Shughrue PJ (2003) Neuroprotection by estrogen in animal models of global and focal ischemia. Ann N Y Acad Sci 1007:89–100 [PubMed: 14993043]

52. Lidegaard O, Edstrom B, Kreiner S (2002) Oral contraceptives and venous thromboembolism: a five-year national case-control study. Contraception 65:187–196 [PubMed: 11929640]
53. Cox A, Varma A, Barry J, Vertegel A, Banik N (2015) Nanoparticle estrogen in rat spinal cord injury elicits rapid anti-inflammatory effects in plasma, cerebrospinal fluid, and tissue. J Neurotrauma 32:1413–1421 [PubMed: 25845398]
54. Gabizon A, Martin F (1997) Polyethylene glycol-coated (pegylated) liposomal doxorubicin. Rationale for use in solid tumours. Drugs 54 Suppl 4:15–21
55. Chvatal SA, Kim YT, Bratt-Leal AM, Lee H, Bellamkonda RV (2008) Spatial distribution and acute anti-inflammatory effects of Methylprednisolone after sustained local delivery to the contused spinal cord. Biomaterials 29:1967–1975 [PubMed: 18255138]
56. Shen Q, Zhang R, Bhat NR (2006) MAP kinase regulation of IP10/CXCL10 chemokine gene expression in microglial cells. Brain Res 1086:9–16 [PubMed: 16635481]
57. Das A, Banik NL, Ray SK (2007) Methylprednisolone and indomethacin inhibit oxidative stress mediated apoptosis in rat C6 glioblastoma cells. Neurochem Res 32:1849–1856 [PubMed: 17570061]
58. Sambandam Y, Townsend MT, Pierce JJ, Lipman CM, Haque A, Bateman TA, Reddy SV (2014) Microgravity control of autophagy modulates osteoclastogenesis. Bone 61:125–131 [PubMed: 24463210]
59. Haque A, Hajiaghamohseni LM, Li P, Toomy K, Blum JS (2007) Invariant chain modulates HLA class II protein recycling and peptide presentation in nonprofessional antigen presenting cells. Cell Immunol 249:20–29 [PubMed: 18067883]
60. Datto JP, Yang J, Dietrich WD, Pearse DD (2015) Does being female provide a neuroprotective advantage following spinal cord injury? Neural Regener Res 10:1533–1536
61. Perot PL Jr, Lee WA, Hsu CY, Hogan EL, Cox RD, Gross AJ (1987) Therapeutic model for experimental spinal cord injury in the rat: I. Mortality and motor deficit. Central Nervous Syst Trauma 4:149–159
62. Satishkumar R, Vertegel AA (2011) Antibody-directed targeting of lysostaphin adsorbed onto polylactide nanoparticles increases its antimicrobial activity against *S. aureus* in vitro. Nanotechnology 22:505103 [PubMed: 22107797]
63. Maximov VD, Reukov VV, Barry JN, Cochrane C, Vertegel AA (2010) Protein-nanoparticle conjugates as potential therapeutic agents for the treatment of hyperlipidemia. Nanotechnology 21:265103 [PubMed: 20534889]
64. Kamaly N, Yameen B, Wu J, Farokhzad OC (2016) Degradable controlled-release polymers and polymeric nanoparticles: mechanisms of controlling drug release. Chem Rev 116:2602–2663 [PubMed: 26854975]
65. Makadia HK, Siegel SJ (2011) Poly lactic-co-glycolic acid (PLGA) as biodegradable controlled drug delivery carrier. Polymers 3:1377–1397 [PubMed: 22577513]
66. Haque MA, Li P, Jackson SK, Zarour HM, Hawes JW, Phan UT, Maric M, Cresswell P, Blum JS (2002) Absence of gamma-interferon-inducible lysosomal thiol reductase in melanomas disrupts T cell recognition of select immunodominant epitopes. J Exp Med 195:1267–1277 [PubMed: 12021307]
67. O'Donnell PW, Haque A, Klemsz MJ, Kaplan MH, Blum JS (2004) Cutting edge: induction of the antigen-processing enzyme IFN-gamma-inducible lysosomal thiol reductase in melanoma cells Is STAT1-dependent but CIITA-independent. J Immunol 173:731–735 [PubMed: 15240658]
68. Haque A, Das A, Hajiaghamohseni LM, Younger A, Banik NL, Ray SK (2007) Induction of apoptosis and immune response by all-trans retinoic acid plus interferon-gamma in human malignant glioblastoma T98G and U87MG cells. Cancer Immunol Immunother CII 56:615–625 [PubMed: 16947022]
69. Hathaway-Schrader JD, Doonan BP, Hossain A, Radwan FFY, Zhang L, Haque A (2018) Autophagy-dependent crosstalk between GILT and PAX-3 influences radiation sensitivity of human melanoma cells. J Cell Biochem 119:2212–2221 [PubMed: 28857256]
70. Haque A, Capone M, Matzelle D, Cox A, Banik NL (2017) Targeting enolase in reducing secondary damage in acute spinal cord injury in rats. Neurochem Res 42:2777–2787 [PubMed: 28508172]

71. God JM, Cameron C, Figueroa J, Amria S, Hossain A, Kempkes B, Bornkamm GW, Stuart RK, Blum JS, Haque A (2015) Elevation of c-MYC disrupts HLA class II-mediated immune recognition of human B cell tumors. J Immunol 194:1434–1445 [PubMed: 25595783]
72. Zhao D, Amria S, Hossain A, Sundaram K, Komlosi P, Nagarkatti M, Haque A (2011) Enhancement of HLA class II-restricted CD4 + T cell recognition of human melanoma cells following treatment with bryostatin-1. Cell Immunol 271:392–400 [PubMed: 21903207]
73. Radwan FF, Zhang L, Hossain A, Doonan BP, God JM, Haque A (2012) Mechanisms regulating enhanced human leukocyte antigen class II-mediated CD4 + T cell recognition of human B-cell lymphoma by resveratrol. Leuk Lymphoma 53:305–314 [PubMed: 21854084]
74. Goldstein OG, Hajiaghamohseni LM, Amria S, Sundaram K, Reddy SV, Haque A (2008) Gamma-IFN-inducible-lysosomal thiol reductase modulates acidic proteases and HLA class II antigen processing in melanoma. Cancer Immunol Immunother CII 57:1461–1470 [PubMed: 18343923]
75. Sribnick EA, Wingrave JM, Matzelle DD, Ray SK, Banik NL (2003) Estrogen as a neuroprotective agent in the treatment of spinal cord injury. Ann N Y Acad Sci 993:125–133; discussion 159–160 [PubMed: 12853305]
76. Zhu P, Zhao MY, Li XH, Fu Q, Zhou ZF, Huang CF, Zhang XS, Huang HL, Tan Y, Li JX, Li JN, Huang S, Ashraf M, Lu C, Chen JM, Zhuang J, Guo HM (2015) Effect of low temperatures on BAX and BCL2 proteins in rats with spinal cord ischemia reperfusion injury. Genet Mol Res GMR 14:10490–10499 [PubMed: 26400280]
77. Bradbury EJ, Burnside ER (2019) Moving beyond the glial scar for spinal cord repair. Nat Commun 10:3879 [PubMed: 31462640]
78. Okada S, Hara M, Kobayakawa K, Matsumoto Y, Nakashima Y (2018) Astrocyte reactivity and astrogliosis after spinal cord injury. Neurosci Res 126:39–43 [PubMed: 29054466]
79. Weil ZM, Gaier KR, Karelina K (2014) Injury timing alters metabolic, inflammatory and functional outcomes following repeated mild traumatic brain injury. Neurobiol Dis 70:108–116 [PubMed: 24983210]
80. Bains M, Hall ED (2012) Antioxidant therapies in traumatic brain and spinal cord injury. Biochim Biophys Acta 1822:675–684 [PubMed: 22080976]
81. Valko M, Leibfritz D, Moncol J, Cronin MT, Mazur M, Telser J (2007) Free radicals and antioxidants in normal physiological functions and human disease. Int J Biochem Cell Biol 39:44–84 [PubMed: 16978905]
82. Nita M, Grzybowski A (2016) The role of the reactive oxygen species and oxidative stress in the pathomechanism of the age-related ocular diseases and other pathologies of the anterior and posterior eye segments in adults. Oxid Med Cell Longev 2016:316473
83. Panieri E, Santoro MM (2016) ROS homeostasis and metabolism: a dangerous liason in cancer cells. Cell Death Dis 7:e2253 [PubMed: 27277675]
84. Kim GH, Kim JE, Rhie SJ, Yoon S (2015) The role of oxidative stress in neurodegenerative diseases. Exp Neurobiol 24:325–340 [PubMed: 26713080]
85. Kamata H, Honda S, Maeda S, Chang L, Hirata H, Karin M (2005) Reactive oxygen species promote TNFalpha-induced death and sustained JNK activation by inhibiting MAP kinase phosphatases. Cell 120:649–661 [PubMed: 15766528]
86. Andersen JK (2004) Oxidative stress in neurodegeneration: cause or consequence? Nat Med 10(Suppl):18–25
87. Shukla V, Mishra SK, Pant HC (2011) Oxidative stress in neurodegeneration. Adv Pharmacol Sci 2011:572634 [PubMed: 21941533]
88. Cheng F, Shen Y, Mohanasundaram P, Lindstrom M, Ivaska J, Ny T, Eriksson JE (2016) Vimentin coordinates fibroblast proliferation and keratinocyte differentiation in wound healing via TGFbeta-Slug signaling. Proc Natl Acad Sci USA 113:E4320–E4327 [PubMed: 27466403]
89. Li X, Li M, Tian L, Chen J, Liu R, Ning B (2020) Reactive astrogliosis: implications in spinal cord injury progression and therapy. Oxid Med Cell Longev 2020:9494352 [PubMed: 32884625]
90. Fitch MT, Silver J (2008) CNS injury, glial scars, and inflammation: Inhibitory extracellular matrices and regeneration failure. Exp Neurol 209:294–301 [PubMed: 17617407]

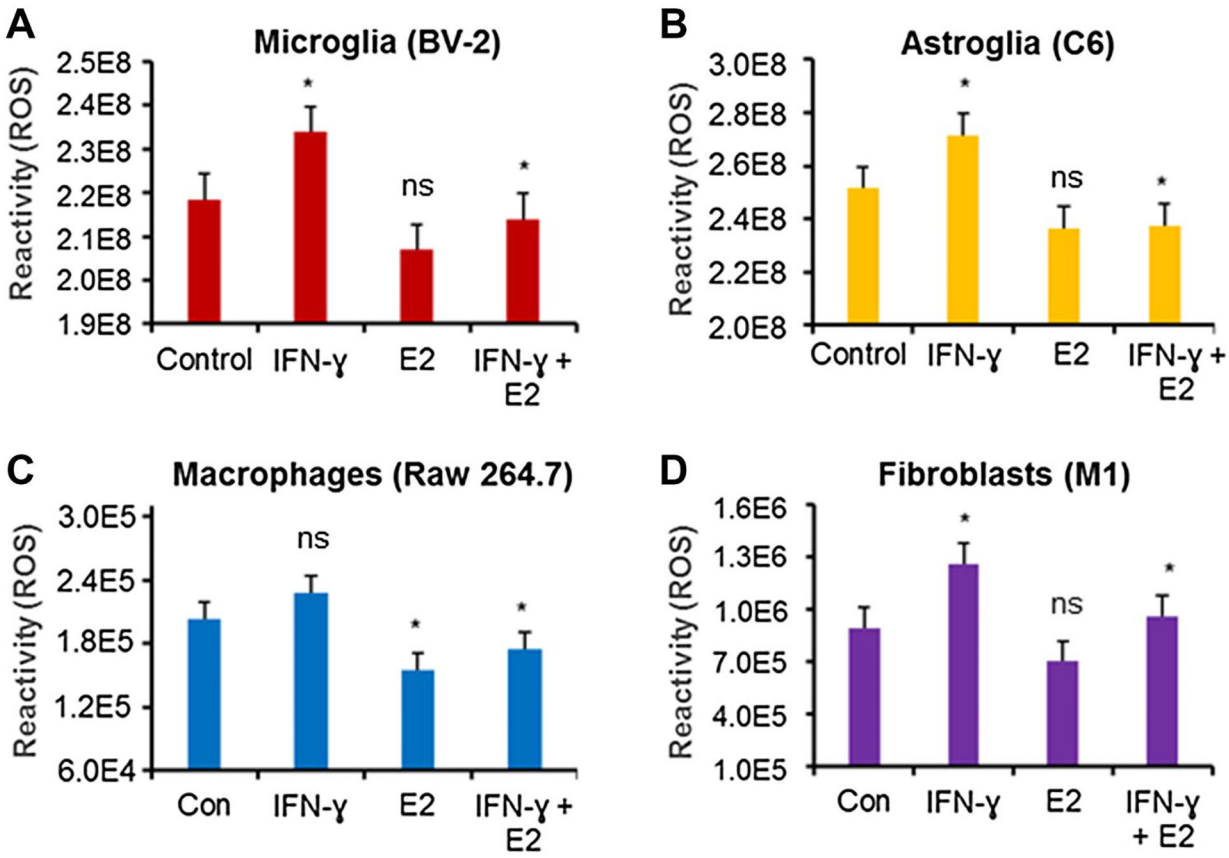

Fig. 1.

Low dose E2 inhibits ROS production by microglia, astroglia, macrophages, and fibroblast cells. BV-2 microglia (**A**), C6 astroglia (**B**), Raw264.7 macrophages (**C**), and M1 fibroblast (**D**) cells were treated with either 40 ng/mL IFN-γ or 40 ng/mL IFN-γ + 40 nM E2 overnight. ROS assay was performed in 96-well plate by the Reactive Oxygen Species Assay Kit (ab113851) according to the manufacturer's protocol. *$p < 0.05$; control vs. IFN-γ, IFN-γ vs. IFN-γ + E2. ns = not significant. Data are representative of three separate experiments

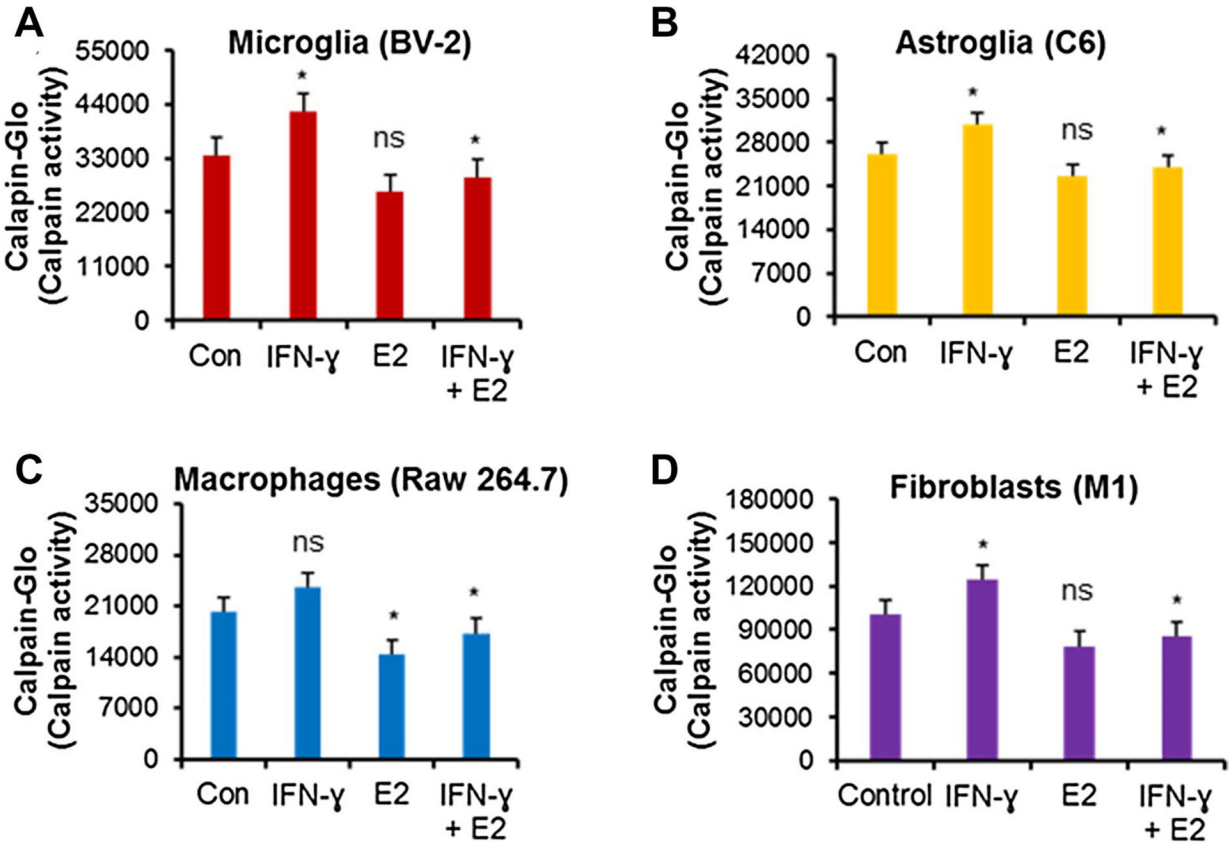

Fig. 2.

Low-dose E2 inhibits calpain activity in microglia (**A**), astroglia (**B**), macrophages (**C**), and fibroblast (**D**) cells. BV-2 microglia, C6 astroglia, Raw264.7 macrophages, and M1 fibroblast cells were treated with either 40 ng/mL IFN-γ or 40 ng/mL IFN-γ + 40 nM E2 overnight. Calpain activity was tested in 100 μg of protein from each group and determined by Calpain-Glo™ Protease Assay Kit (G8501) according to the manufacturer's protocol. *$p < 0.05$; control vs. IFN-γ, IFN-γ vs. IFN-γ + E2. ns = not significant. Data are representative of three separate experiments

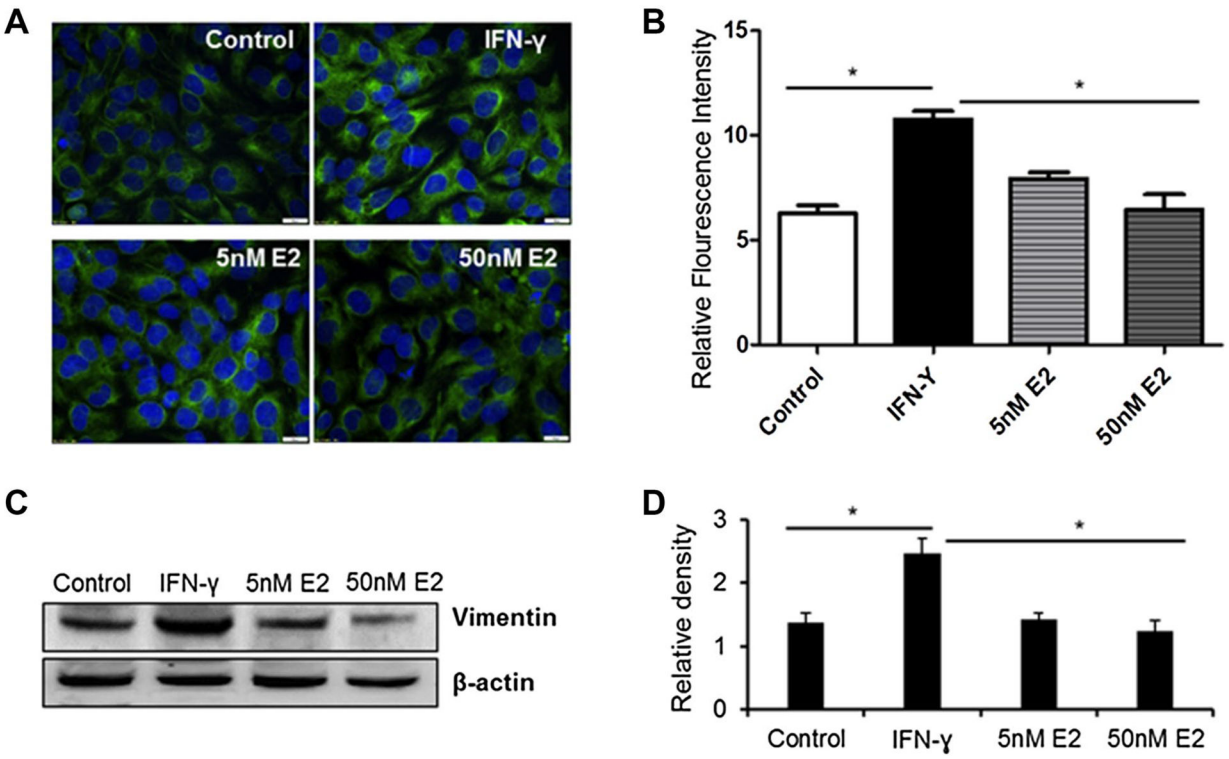

Fig. 3.

Low-dose E2 inhibits vimentin protein expression by human fibroblast cells. Human fibroblast cell line M1 was treated with 40 ng/mL of IFN-γ or 40 ng/mL of IFN-γ plus 5–50 nM of E2 overnight at 37 °C. (**A**) Immunofluorescence assay was performed as described in the methods. (**B**) Relative immunofluorescence intensity was quantitated by ImageJ software (*$p < 0.05$; Control vs. IFN-γ and IFN-γ vs. E2). (**C**) Western blot analysis of vimentin using anti-vimentin antibody (ab92547). (**D**) Densitometric analysis of protein band intensity by ImageJ (*$p < 0.05$). Data are representative of three separate experiments

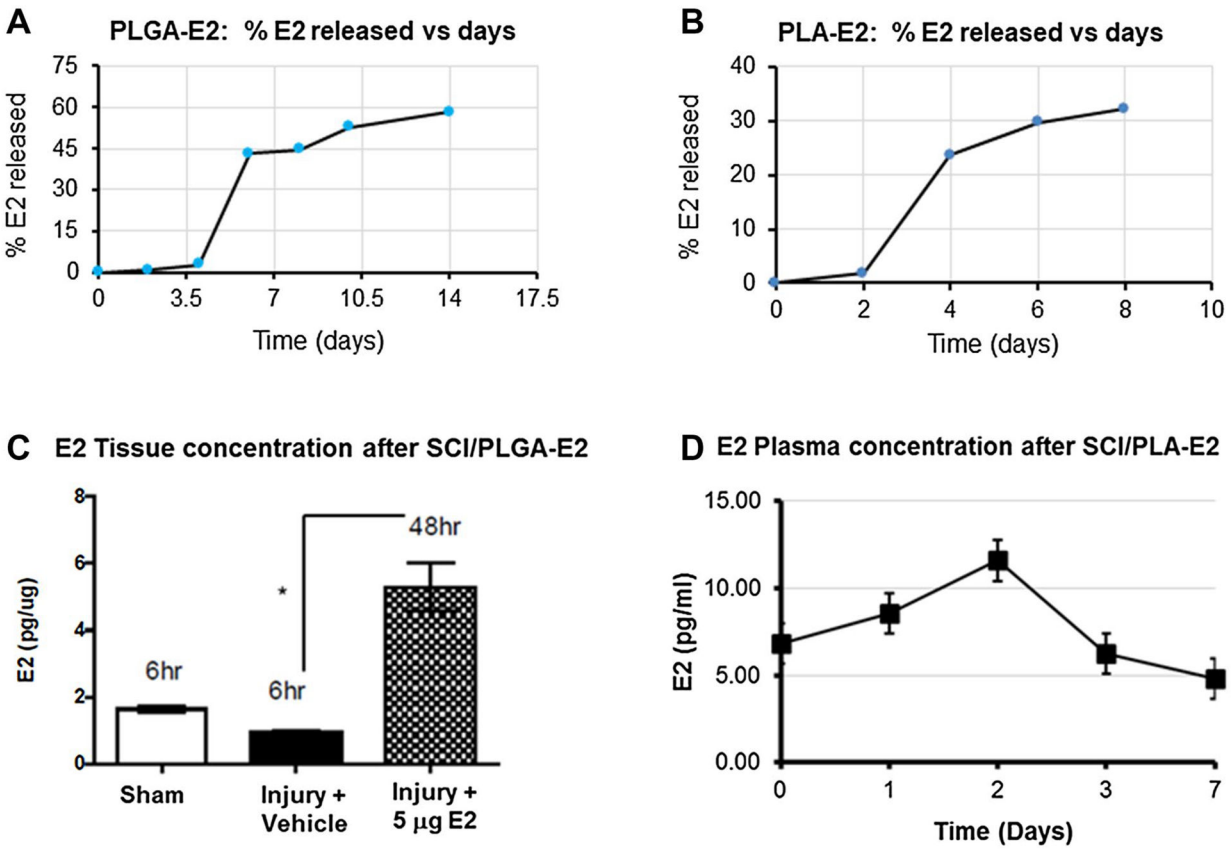

Fig. 4.

Availability of E2 from fast and slow release nano-E2 therapy following SCI. (**A)** Percent E2 released from PLGA-E2 in vitro over time. (**B)** Percent E2 released from PLA-E2 in vitro over time. (**C)** SCI rats were treated with PLGA-E2 (5 µg), and spinal cords were collected at 6 and 48 h post injury. Tissues were homogenized and E2 concentration was measured by ELISA (Calbiotech ES180S). (**D)** SCI rats were treated with PLA-E2 (5 µg), and plasma samples were collected at various time points after SCI and analyzed by ELISA. *$p < 0.05$. N = 3–5

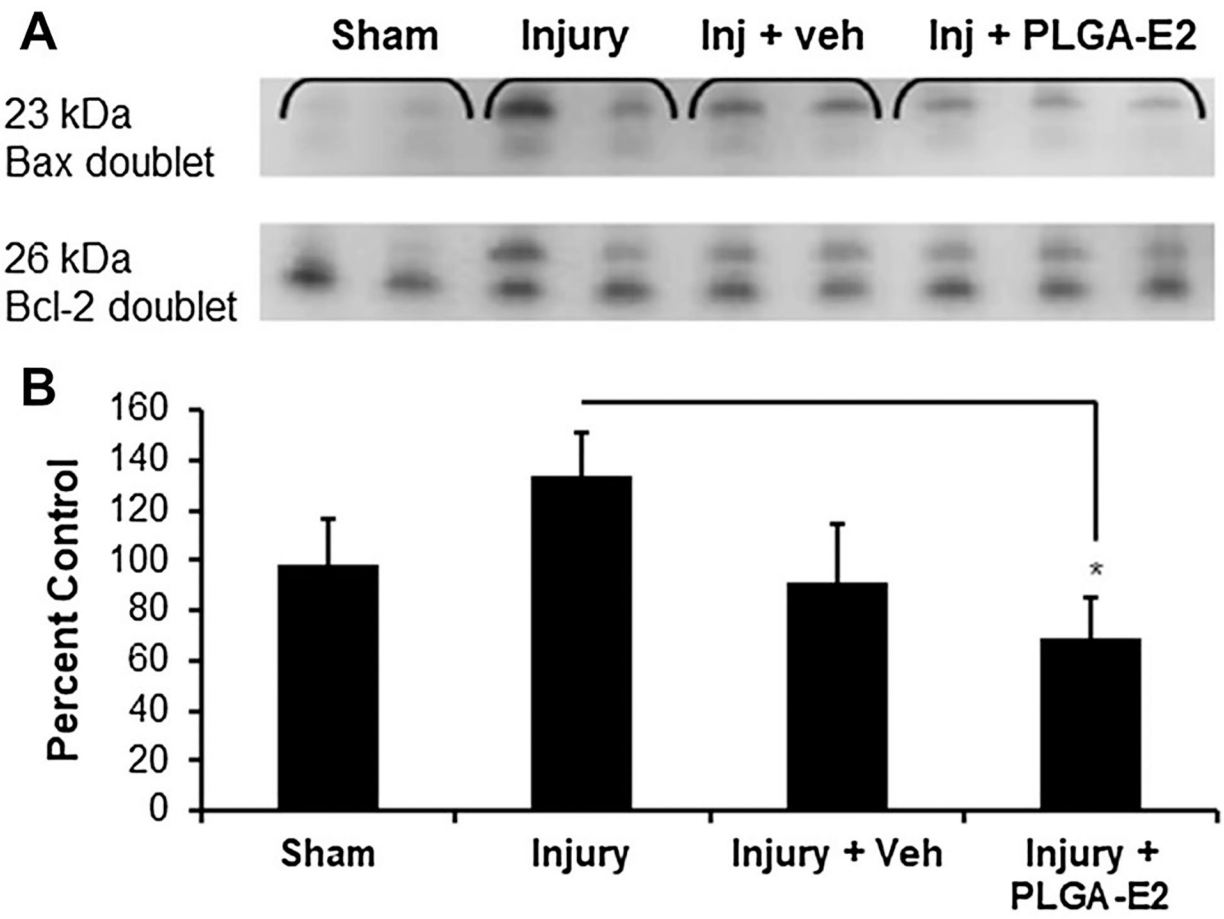

Fig. 5.

SCI rats were treated with PLGA-E2 for 48 h. (**A)** Spinal cord tissues from lesion section were obtained, homogenized, and subjected to western blotting for Bax and Bcl-2. (**B)** Densitometric analysis of protein band intensity and a ratio of Bax and Bcl-2 suggest 30% increase with injury, but a significant decrease after PLGA-E2 treatment (*$p < 0.05$ Injury + PLGA-E2 vs. Injury. N = 3 in sham group, and N = 5 in injured groups)

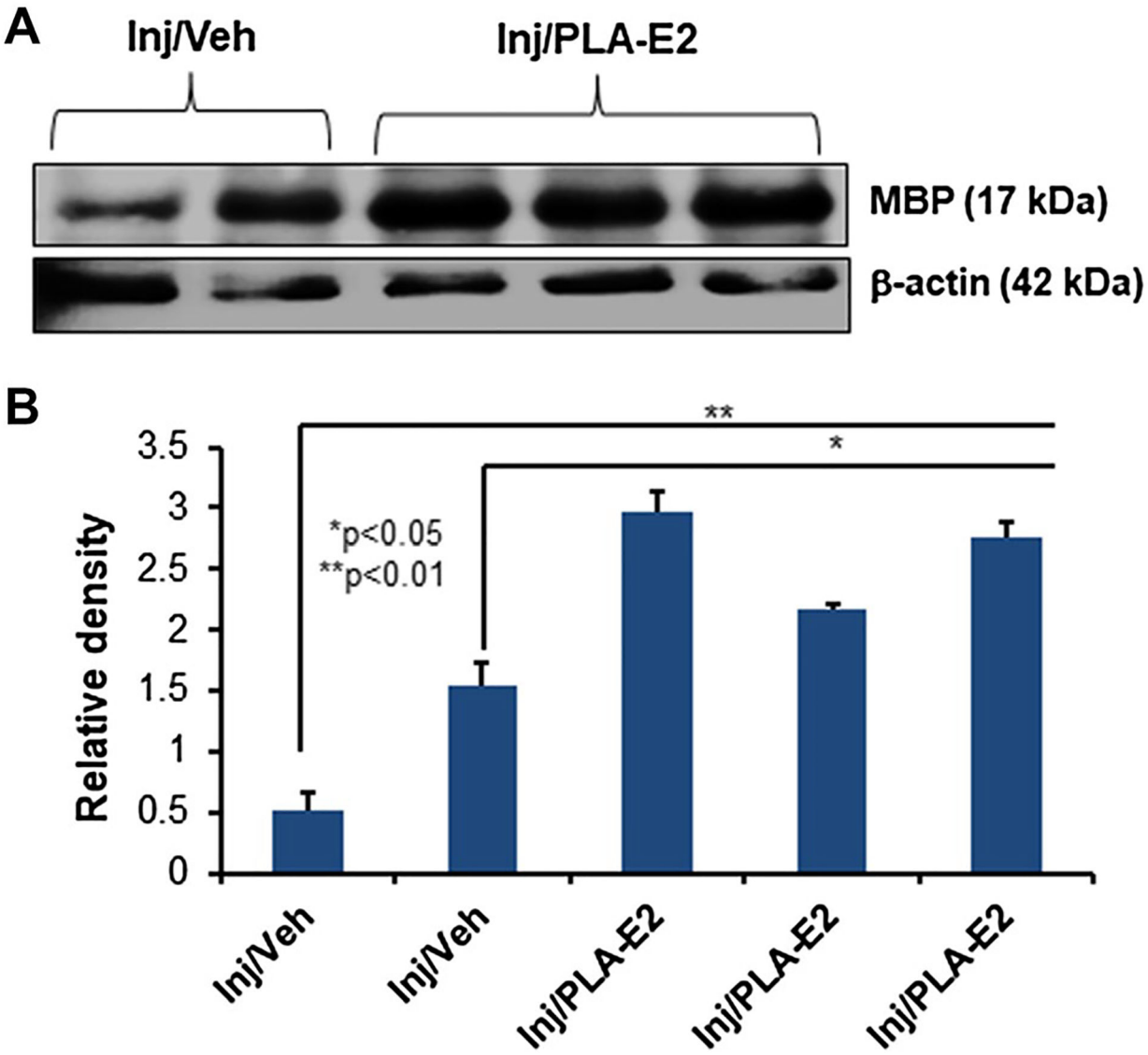

Fig. 6.

SCI rats were treated with PLA-E2 for 7–14 days as described. (**A)** Spinal cord tissues distal to the lesion section were obtained, homogenized, and subjected to western blotting for MBP. (**B)** Densitometric analysis of protein band intensity suggests a significant increase in MBP protein expression after PLA-E2 treatment (N = 3–5)

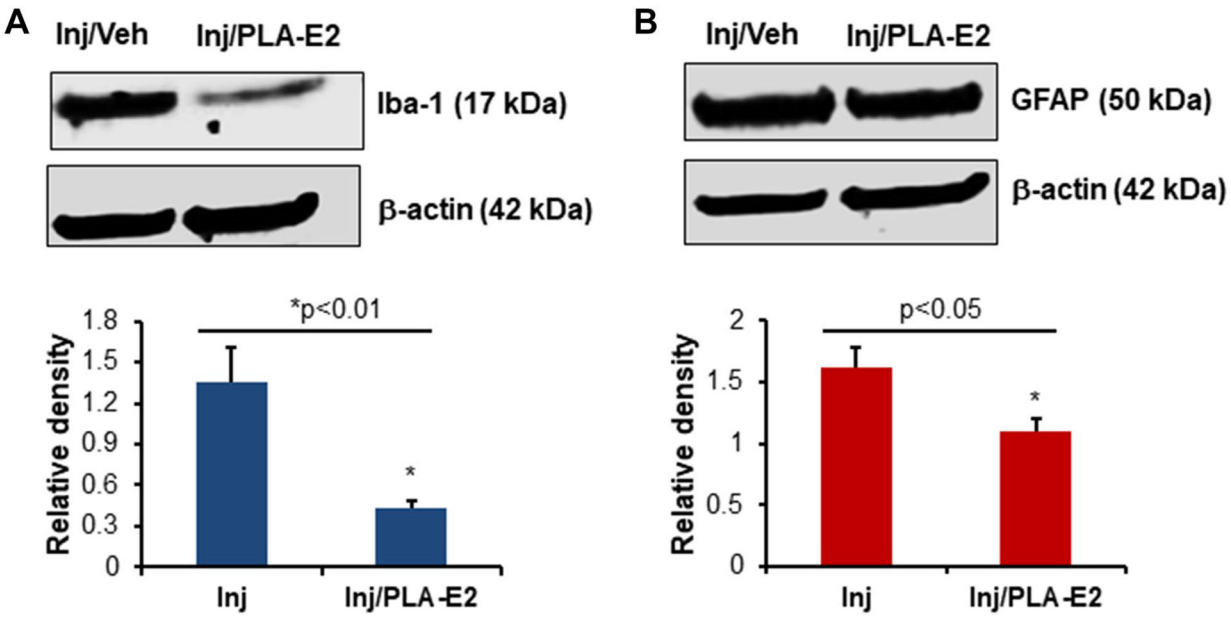

Fig. 7.

Rats were treated with PLA-E2 (5 μg), and spinal cords were collected at seven days post injury. Tissues were homogenized and analyzed by western blotting for Iba-1 (**A**) and GFAP (**B**) as described in the methods. Densitometric analysis of protein band intensity (lower panels) suggests that Iba-1 and GFAP expression levels were significantly inhibited by PLA-E2 treatment (N = 3–4 per group)